

Physical activation of waste-derived materials for biogas cleaning

*Original*

Physical activation of waste-derived materials for biogas cleaning / Papurello, Davide; Santarelli, Massimo; Fiorilli, Sonia.  
- In: ENERGIES. - ISSN 1996-1073. - 11:9(2018), p. 2338. [10.3390/en11092338]

*Availability:*

This version is available at: 11583/2728423 since: 2019-03-15T07:40:17Z

*Publisher:*

MDPI AG

*Published*

DOI:10.3390/en11092338

*Terms of use:*


This article is made available under terms and conditions as specified in the corresponding bibliographic description in the repository

*Publisher copyright*

(Article begins on next page)

Article

# Physical Activation of Waste-Derived Materials for Biogas Cleaning

Davide Papurello <sup>1,\*</sup> , Massimo Santarelli <sup>1</sup> and Sonia Fiorilli <sup>2</sup>

<sup>1</sup> Department of Energy (DENERG), Politecnico di Torino, Corso Duca degli Abruzzi, 24, 10129 Turin, Italy; massimo.santarelli@polito.it (M.S.); Sonia.fiorilli@polito.it (S.F.)

<sup>2</sup> Department of Applied Science and Technology (DISAT), Politecnico di Torino, Corso Duca degli Abruzzi, 24, 10129 Turin, Italy

\* Correspondence: davide.papurello@polito.it or papurello5@gmail.com; Tel.: +39-340-235-1692

Received: 25 May 2018; Accepted: 30 August 2018; Published: 5 September 2018



**Abstract:** Biogas produced from biomass is carbon neutral. In fact, the carbon feedstock of biomass is converted into gas phase. Biogas use in high efficient energy systems, such as Solid Oxide Fuel Cells is a viable choice. One of the most important drawbacks for such systems is related to the interaction between trace compounds and anode section. Gas cleaning through physical removal mechanisms is the simplest and cheapest method adopted in the literature. Coupled with this solution, the recovery of waste materials is an efficient application of the circular economy approach. In this work, a physical activation process was investigated experimentally for waste-derived materials at a temperature of 700 °C. The removal of H<sub>2</sub>S was considered as the most abundant trace compound. Activated biochar showed an adsorption capacity comparable to commercial sorbents, while the performance of ashes are still too poor. An important parameter to be considered is the biogas humidity content that enters in competition with trace compounds that must be removed.

**Keywords:** waste-derived materials; biogas; adsorption; physical activation

## 1. Introduction

Scientists believed that the Earth's climate change could be related to the high concentration of CO<sub>2</sub> and other greenhouse gases produced by human activities. How biogas can reduce or mitigate this problem is a scientific challenge. Biogas produced from biomass is considered to be carbon neutral, since the carbon feedstock of biomass is converted into gas phase. In other words, atmospheric carbon (CO<sub>2</sub>) is captured in a relatively short time. Biogas is a secondary energy carrier and can be produced from many organic substrates, such as from agricultural sources, sewage sludge and animal waste [1–6]. In addition to the chemical process, a thermal process (gasification or pyrolysis) can exploit organic material for biogas production purposes. The European Biomass Organisation for 2020 estimated a production of biogas around 39.5 Mtoe, which corresponds to 10% of EU natural gas consumption [7]. Biogas can be adopted as a fuel for several energy generators, such as fuel cells, as well as external and internal combustion engines [8,9]. Alternatively, biogas can be upgraded with highly engineered systems into biomethane to be injected into the gas grid [10,11]. Among energy generators, high temperature solid oxide fuel cells have higher electrical efficiency values, high fuel feeding flexibility, low noise and pollutant emissions [8,12–14]. The most important drawbacks for such generators is the low tolerability to trace compounds [3,15–22]. Depending on the nature of the trace compound and its concentration in the gaseous matrix, a gas cleaning section has to be specifically designed. The most frequently detected trace compounds from Organic Fraction of Municipal Solid Waste (OFMSW) biogas are sulphurs, carbonyl compounds, carboxylic acids and terpenes [2,4]. Rasi et al. (2011) studied the trace compounds that affect biogas energy users [6]. They mainly

detected halogens, aromatic and sulphur compounds in landfill gas. In addition, they detected sulphur compounds, aromatic and siloxane in biogas from the sewage sludge digestion and from waste water treatment plants [6]. Physical adsorption removal using commercially available activated carbons has been investigated in several studies [23–26]. Its possible use will be determined by economic evaluation based on factors such as its performance and its production cost [27]. The high removal performance of these materials is related to their physical and chemical characteristics. Their specific surface area, the micropore and mesopore volume, as well as the impregnating agents adopted for their chemical activations are also important [27–29]. Generally, alkali metals are adopted to improve removal performance, such as potassium, but also alkaline earth metals, such as calcium and magnesium. Barelli et al. (2017) showed how the choice of the impregnating agent is important in the removal of sulphur compounds. In fact, when the carbon is activated with KI and KOH, the role of water on the adsorption capacity has a positive effect [30]. In Papurello et al. (2016) this effect was not highlighted due to the absence of such agents and the role of water remained negative [31]. Another parameter to be considered in literature is the removal of contemporary pollutants. In literature there are several papers that study the interaction of trace compounds with the sorbent materials, such as: Aromatic, terpenes and carboxyls with sulphur compounds [25,26,32–35]. Waste materials recovery is an efficient application of the circular economy approach. This approach reduces waste and pollutants. Thermo-chemical processes are applied to biomass, as reported in literature using pyrolysis or gasification systems [36]. Pyrolysis process produces char and oil, with a high potential for recovering energy [37,38]. Another waste material suitable for the gas cleaning of biogas is wood ash [39]. Wood ash is an attractive solution due to the low cost of disposal [39]. Ducom et al. (2013) showed how fly ash from biomass was able to remove some trace compounds from the biogas [40]. Fly ash from wood waste and char have a lower removal capacity for the desulphurisation of biogas compared to commercially activated carbons [39,41–44]. The waste materials adopted for the purpose of cleaning biogas require more research, especially on the improvement of their physical characteristics, such as microporous volume and specific surface area. In this work, a physical activation process is investigated for SOFC gas requirements. The removal of H<sub>2</sub>S, considered to be the most abundant sulphur compound from a simulated biogas mixture, was investigated.

## 2. Experimental Methods

### 2.1. Description of the Experimental Setup

The pyrolysis of wood waste produces a biochar that Gruppo RM Impianti srl (Arezzo, Italy) exploit internally. The reactor adopted is 200 kW<sub>e</sub> with operating temperature of around 450 °C (construction details reserved). Ashes from wood-chips from local forest were obtained from a boiler (3.3 MW, Viessman, Allendorf, Germany). The activation of biochar and wood ash was accomplished using an electric furnace of 500 We (C.I.T.T., Milano, Italy) regulated with a PID controller (Horst, GmbH Germany). Technical instructions are reported as follows: heat-up ramp fixed at 7 °C/min until 700 °C, with a CO<sub>2</sub> flow rate of 100 mL/min, see Figure 1a. The physical activation step was carried out for a period of 60 min under isothermal conditions. The operating temperature for the reactor was fixed using a furnace regulated by a K-type thermocouple placed in the centered bed. Two additional thermocouples (K-type, Tersid, Italy) were placed at the outlet and inlet of the bed. Experiments were accomplished with a Gas Hourly Space Velocity (GHSV) of 66 h<sup>-1</sup>.

Figure 1b depicts the sorbent material testing set-up. A simulated biogas mixture was accomplished (CH<sub>4</sub>/CO<sub>2</sub> = 1.5) using gas cylinders (Siad spa, Praxair with mass and liquid flow controllers (MFC, LFC) (Bronkhorst GmbH, Ruurlo, The Netherlands). A controlled evaporator mixer (CEM) was adopted to add water to the heated lines with a relative humidity of 30% (RH). A gas mixture prepared with CO<sub>2</sub> and H<sub>2</sub>S (190 ppm(v)) was used for the removal of trace compounds. The H<sub>2</sub>S concentration was fixed at 75.9 ppm(v) and obtained from the dilution with pure CO<sub>2</sub>, in order to simulate an average biogas mixture deriving from the anaerobic digestion of organic waste. This concentration is

representative of a real biogas, as reported in literature [5,44,45]. Biochar and ashes were ground and sieved before and after the activation process, to obtain a grain size around 400  $\mu\text{m}$ . These sorbent materials were placed in Teflon tubes with an internal diameter of 4 mm and an L/D ratio around 10. The removal test was accomplished three times, both for the activated and for the not activated sorbent materials.

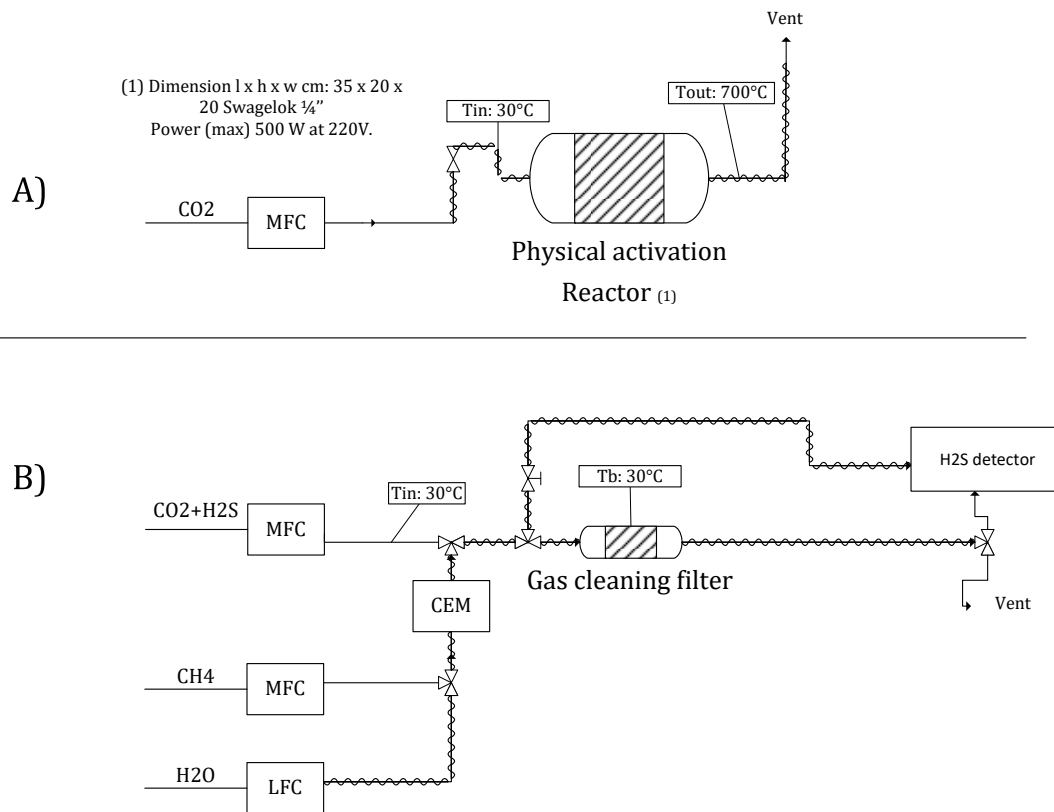


**Figure 1.** Experimental set-up: (a) activation test rig, (b) sorbent material testing for VOCs removal.

## 2.2. Methodology

In order to maintain the correct aspect ratio ( $\sim 4$ ) between the pellet and reactor diameter, the sorbents were ground and sieved [46]. This procedure was followed before the activation process. The testing sample was selected using metallic sieves in the range 5.4–400  $\mu\text{m}$ . In supplementary material, the pore distribution of activated carbons and waste-derived materials are reported. To remove residual gases inside the pores the samples were pre-treated using  $\text{N}_2$  flow (200  $\text{NmL}/\text{min}$ ) for 30 min at 120  $^\circ\text{C}$ . A gas flow of 200  $\text{NmL}/\text{min}$  was used for the removal performance testing. Dynamic tests for the sulphur removal were accomplished for the selected materials at 25  $^\circ\text{C}$ . Below the adsorption capacity equation is reported, calculated in terms of  $\text{mg}/\text{g}$  for  $\text{H}_2\text{S}$  removal:

$$C_{ads} = \frac{Q_{tot} \cdot MW \cdot [c_{in} \cdot t_1 - (t_1 - t_0) \cdot 0.5]}{V_m \cdot m \cdot 10^3} \quad (1)$$

where:

- $t_0$ , is the cleaning service time;
- $t_1$ , is the last detection interval, corresponding to initial concentration for  $\text{H}_2\text{S}$  of 1%, 10% and 100%;
- $Q_{tot}$  = total gas flow rate ( $\text{NL}/\text{h}$ );
- $MW$  = molecular weight of the trace compound removed ( $\text{g}/\text{mol}$ );

- $C_{in}$  = inlet trace compound concentration (ppm(v));
- $V_m$  = molar volume (22.414 NL/mol);
- $m$  = mass of sorbent (g).

Considering the work of Barelli et al. (2016), Equation (1) was adjusted. In fact, the difference between the rectangle ( $t_1$  (h)  $\times C_{in}$  (ppm(v))) and the triangle areas ( $0.5(t_1 - t_0)$  (h)  $\times 1$  (ppm(v))) approximates the area enclosed by the breakthrough curve and the saturation line ( $C_{out} = C_{in}$ ) [47]. An electrochemical gas sensor (ES, Meccos eTr—Leopold Siegrist GmbH, Lorsch, Germany) was adopted to measure the H<sub>2</sub>S concentration. This sensor is able to perform a continuous reading in the range of 0–200 ppm(v). The accuracy of the sensor reading is 0.5%, while a value of 1% is fixed for the electrochemical sensor. Flow meter controllers have an accuracy value of 0.1%, related to the full-scale value.

### 3. Results and Discussion

Results related to the adsorption capacity were reported below, starting from the characterization to the sorbent selection considering also the waste-derived materials.

#### 3.1. Sorbent Characterisation—EDS/SEM

The sorbent materials adopted were characterised in terms of their surface area, composition, micropore volume and morphology structure. The elemental composition measurements were performed by scanning electron microscopy (SEM) (FEI Inspect, Philips 525 M) coupled with EDS analysis (SW9100 EDAX). The results are reported in Table 1, nitrogen and hydrogen fractions are not reported due to the limits of the instrument.

The most abundant compound for biochar samples is carbon followed by oxygen, potassium, calcium, and magnesium. The activation process does not substantially modify the elemental composition. A decrease in potassium content with a corresponding increase in calcium content was recorded. The most abundant compound for the ash samples is oxygen, followed by silicon, carbon, potassium, calcium, magnesium and aluminium. The activation process does not substantially change the elemental composition.

Tepper and Richardson et al. (2002) demonstrated how the concentrations of K and Ca are important for the sulphur compound removal [48,49]. Transition metals are also important for salt formation with trace compounds.

**Table 1.** Composition in terms of weight fraction for the materials tested.

	Biochar	Activated Biochar	Ash	Activated Ash	Commercial Carbon (RST3)	Commercial Carbon (Carbox)	ZnO
C	77.5	81.8	14.26	14.8	91.1	80.9	
O	13.98	16.65	49.29	49.4	5.3	9.01	24.79
Si			23.73	22.2		1.4	0.55
Al			0.60	0.59		1.98	0.96
K	0.93	0.33	9.99	10.75	0.79	0.78	
Ca	0.90	1.63	1.3	1.4	0.75	1.65	0.75
Mg	0.24	0.19	0.62	0.64	0.31	1.19	
Cl			0.21	0.22		0.33	
P						0.81	
S					0.59	0.11	
Mn						0.41	
Fe						1.43	
Zn					1.16		72.95

The adsorption isotherms were determined using a Quantachrome Autosorb 1 (Boynton Beach, FL, USA) using for N<sub>2</sub> at 77 K. The specific surface areas were calculated by Langmuir equation in the relative pressure range of 0.04–0.1. The micropore volumes were determined by means of t-plot method in the relative pressure range of 0.15–0.3. For the carbon-based materials, the pore size was

evaluated through the DFT method (Density Functional Theory), using the NLDFT equilibrium model for slit/cylindrical pores, see Table 2.

**Table 2.** Surface and volume characteristics for the materials tested.

		Biochar	Activated Biochar	Ash	Activated Ash	Commercial Carbon (RST3)	Commercial Carbon (Carbox)	ZnO
Specific surface area	(m <sup>2</sup> /g)	75	593	0.9	6	1117	1237	35.8
Microporous volume	(cm <sup>3</sup> /g)	0.04	0.26	0.01	0.07	0.3	0.328	
Total pore volume	(cm <sup>3</sup> /g)	0.06	0.37	0.015	0.1	0.447	0.407	0.196

The isotherm graph recorded for the biochar, according to IUPAC classification, is of type I. Such isotherm is typical of microporous materials. In Figure 2 the sharp increase in adsorbed volume at low relative pressures is depicted. This is due to the capillary condensation of the adsorbate inside the micropore. The presence of a hysteresis loop suggests the presence of slit porosities, due to the particles aggregation.

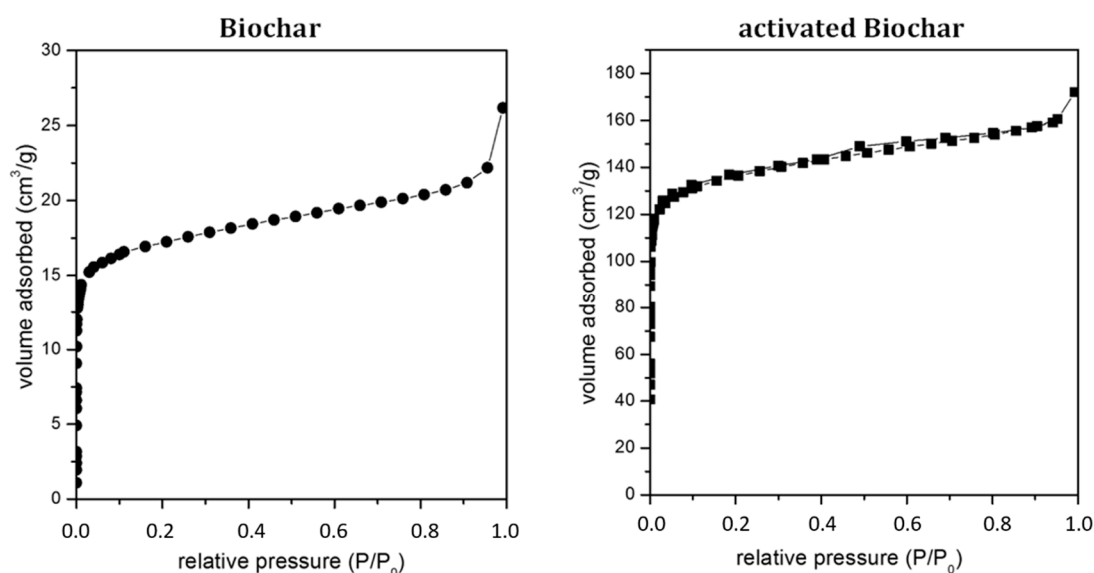


**Figure 2.** Isotherm graph recorded for biochar characterization, according to IUPAC classification.

In the following Figure 3, an analysis to SEM images is necessary for the sorbent materials adopted, on the left side before activation and on the right side after the activation process.

The waste-derived biochar and ash were physically activated at a fixed temperature and CO<sub>2</sub> flow rate. The structure before this physical process was denser and the homogeneity of the structure cannot be guaranteed by the un-optimized production phase. At the end of the activation process, especially for the biochar sample, the increase of porosity and consequently the specific surface area value was evident. This value after the activation process was around 600 m<sup>2</sup>/g, while the micro pore volume ranged from 0.04 cm<sup>3</sup>/g to 0.26 cm<sup>3</sup>/g; and the total volume ranged from 0.06 cm<sup>3</sup>/g to 0.37 cm<sup>3</sup>/g. The ash sample was activated using the same process. The specific surface increased to 6 m<sup>2</sup>/g, while the micro pore and total pore volume also increased according to a similar ratio recorded for the biochar.



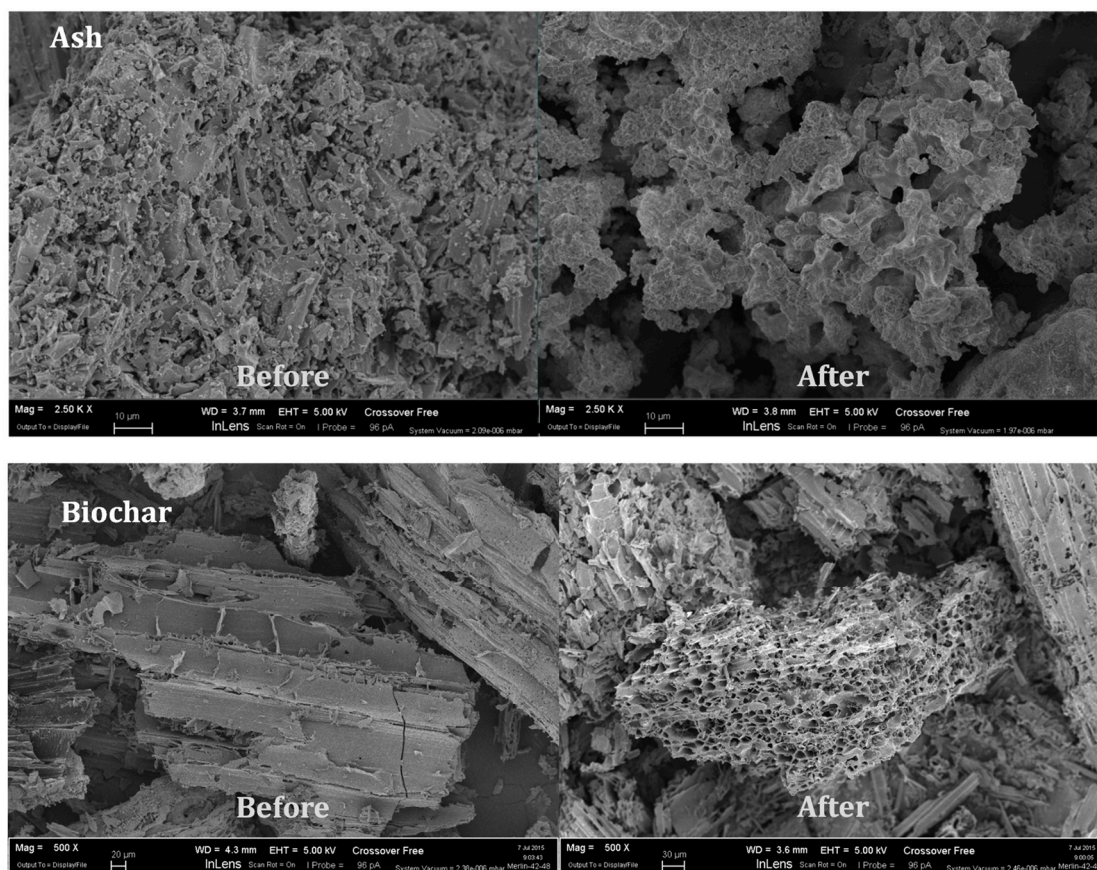


**Figure 3.** Scanning electron microscopy images for the materials tested – before and after the physical activation process.

### 3.2. Adsorption Capacity

The recovery of waste materials is an interesting application of the circular economy approach. In fact, literature studies consider a wide range of wastes, such as from agricultural sector for the production of activated carbons [50]. In this work two waste-derived materials have been selected, such as char from the pyrolysis of wood waste, and ashes from the combustion of wood chips in a boiler. Virgin chars, as reported also in this article have lower adsorption capacity for the removal of trace compounds, especially sulphur compounds [37]. The activation methods are divided into chemical and physical origin. Due to technical simplicity and economical aspects, physical activation was adopted as the activation method for the sorbent materials removal of sulphur compounds [51–53]. The pore size distribution and pore fraction of the activated biochar vary according to the quantity and type of biomass, operating temperature and activating gas [54]. According to Nabais et al. (2007), the CO<sub>2</sub> activation leads to samples with higher BET surface areas and pore volumes compared with samples produced by steam activation and with similar burn-off values [55]. Zhang et al. (2004) studied the duration of CO<sub>2</sub> activation and temperature on the characteristics of the char produced from the wood fast pyrolysis [56]. Chars type selected showed an increasing of specific surface area and micropore volume with increasing activation temperature. The increasing of pore size and surface area was verified up to 900 °C, above this value the carbon characteristics decrease [57].

Table 3 shows the adsorption capacity for commercial carbons and waste-derived materials for the removal of H<sub>2</sub>S. Commercial carbons have an adsorption capacity of around 2 mg/g while commercial metal oxides, such as ZnO has an average removal capacity of around 1 mg/g at  $t_1 = 1\%$  of initial concentration. The two commercial carbons selected have a similar adsorption capacity also at the saturation condition,  $t_1 = 100\%$ . Carbox compared to RST3 shows a steeper profile for the removal

of H<sub>2</sub>S. Waste derived materials not physically activated show an adsorption capacity lower than commercial materials. Here, the surface area and microporous volume weight strongly on the removal performance, as reported [58]. In fact, as reported in the following Figure 4, the adsorption capacity is directly correlated to the specific surface area and microporous volume. Higher micropore volume along with smaller pores results in enhanced capacity of H<sub>2</sub>S removal. As reported by Adib et al. (2000), the mesoporous volume seems less important for the adsorption capacity performance [59].

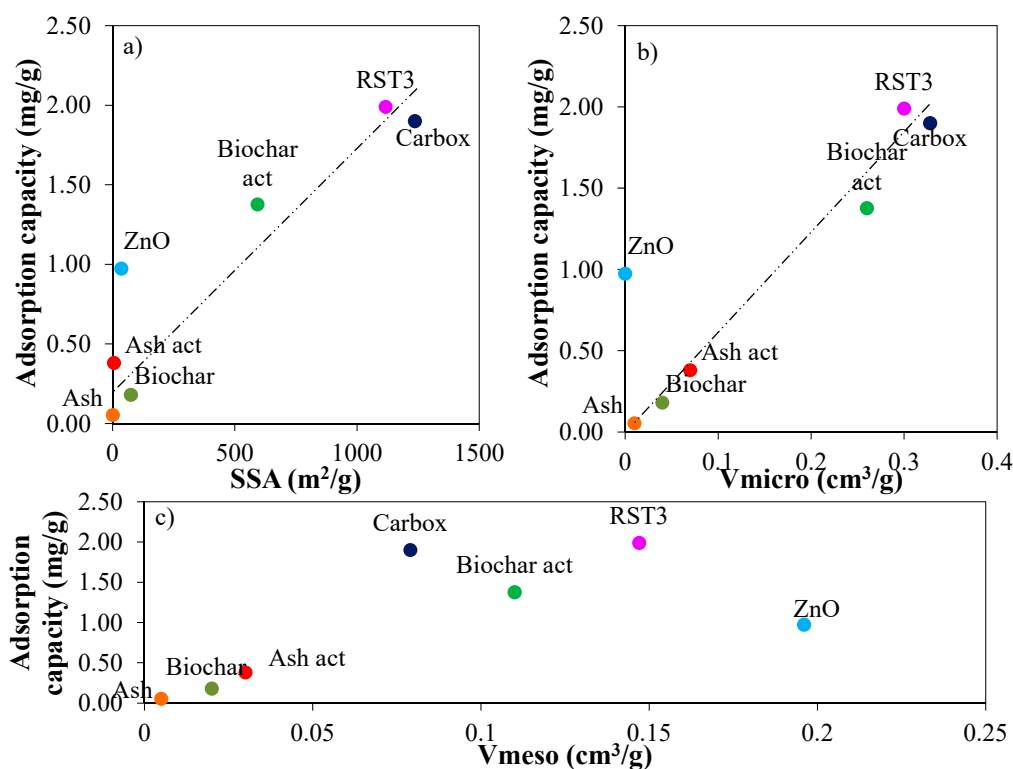


**Figure 4.** Adsorption capacity in relation with surface area and microporous volume: (a) SSA vs. Cads.; (b) V<sub>micro</sub> vs. Cads.; (c) V<sub>meso</sub> vs. Cads.

In Figure 4, the coefficient of determination is higher than 0.95 for surface area and adsorption capacity, while this coefficient is higher than 0.98 for microporous volume and adsorption capacity. ZnO sample, as reported in the characterization section is defined by an adsorption isotherm related to chemical mechanisms, demonstrated by not observing the linear correlation reported in Figure 4. This removal mechanism is stronger than physisorption, both for removal and regeneration of material. To explain these poor performances, Aravind et al. (2012) demonstrated how the optimal metal oxides performances are shown at a higher temperature [60].

**Table 3.** Adsorption capacity for waste-derived materials and commercial carbons for H<sub>2</sub>S removal.

Sorbent	Load (g)	Cads. (mg/g)-1%			Std. Dev	Cads. (mg/g)-10%			Std. Dev	Cads. (mg/g)-100%			Std. Dev
Commercial sorbents													
Airdep	0.53	1.88	1.88	1.94	0.03	6.75	6.74	6.77	0.01	12.45	12.54	12.65	0.08
CarbOx													
Norit RST3	0.3	1.95	2.04	1.98	0.04	2.76	2.81	2.83	0.03	12.10	12.11	12.17	0.03
Zinc oxides	0.33	0.92	0.98	1.02	0.04	24.74	24.75	24.81	0.03	47.07	47.17	47.21	0.06
Waste derived materials													
Biochar	0.25	0.12	0.19	0.23	0.05	0.27	0.31	0.40	0.05	4.76	4.85	4.92	0.07
Biochar act	0.16	1.30	1.38	1.45	0.06	1.95	2.01	2.11	0.07	9.85	9.89	10.01	0.07
Ash	0.95	0.02	0.06	0.08	0.02	0.16	0.10	0.17	0.03	0.23	0.25	0.27	0.02
Ash act	1.03	0.29	0.37	0.48	0.08	0.65	0.66	0.69	0.02	1.77	1.79	1.75	0.02



The physical activation with CO<sub>2</sub> and higher temperature allows us to improve the average adsorption capacity from 0.18 mg/g to 1.38 mg/g for biochar, and from 0.05 mg/g to 0.38 mg/g for ashes.

As reported by Nabais et al. (2007), physical activation with CO<sub>2</sub> promotes pore size and surface area increasing, with better performance than steam activation [55]. Activated biochar shows an adsorption capacity comparable to commercial sorbents, as reported also from [37,61]. Increasing the saturation zone of the filter, from 1% to 10% up to 100%, the adsorption capacity increases up to the saturation of pores, see Table 3. The latter value is a limit of the filter bed filled by sorbent material. An average value of 10 mg/g was registered for activated biochar. This value is not comparable with those obtained with activated ash, while appears similar with those obtained with activated carbons [39]. Metal oxides are able to promote the dissociation of H<sub>2</sub>S and the HS<sup>-</sup> reaction to form sulphides. These reaction are reported in literature studies, as studied from Shang et al. (2016) [37]. This was due to the chemical mechanisms developed between trace compounds to be removed and metals [62].

Table 4 depicts the adsorption capacity of H<sub>2</sub>S in a wet biogas using commercial activated carbons, waste-derived materials and activated waste-derived materials.

**Table 4.** Adsorption capacity for waste-derived materials and commercial carbons for H<sub>2</sub>S + H<sub>2</sub>O removal.

Sorbent	Load (g)	Cads. (mg/g)-1% + H <sub>2</sub> O (30%)			Std. Dev	Cads. (mg/g)-10% + H <sub>2</sub> O (30%)			Std. Dev	Cads. (mg/g)-100% + H <sub>2</sub> O (30%)			Std. Dev
Commercial sorbents													
Airdep	0.17	1.30	1.37	1.49	0.08	5.19	5.27	5.39	0.08	8.65	8.74	8.78	0.05
CarbOx													
Zinc oxides	0.30	0.34	0.43	0.54	0.08	2.45	2.51	2.62	0.07	29.44	29.48	29.55	0.05
Waste derived materials													
Biochar	0.31	0.01	0.02	0.08	0.03	0.08	0.12	0.13	0.02	2.65	2.69	2.80	0.06
Biochar act	0.28	0.90	0.93	1.04	0.06	1.26	1.29	1.35	0.04	5.93	5.98	6.02	0.04
Ash	1	0.01	0.02	0.04	0.01	0.14	0.15	0.18	0.02	0.26	0.17	0.20	0.04
Ash act	1.04	0.17	0.19	0.25	0.03	0.42	0.47	0.50	0.03	1.10	1.17	1.19	0.04

Biogas water vapor (30% RH) enters into competition with hydrogen sulphide that has to be removed. This competition decreases the adsorption capacity [31]. In fact, as reported elsewhere [31], when the RH value is above 50%, the adsorption capacity tended to be zero. At  $t_1 = 1\%$  of the initial H<sub>2</sub>S concentration, the average adsorption capacity value registered for Carbox decrease from 1.9 mg/g up to 1.39 mg/g. A stronger decrease is obtained using ZnO. In fact, the adsorption capacity in the same conditions decreases of 55%.

Considering waste-derived materials, the effect of water content on the removal performance has the same effect registered for commercial sorbents [63]. Because this material is not activated chemically with alkali metals, water content competes with sulphur for their removal [30]. The adsorption capacities decrease more in the case of not possessing physically activated material. In fact, pores and surface area being lower suffer more from the competition of water content. Biochar shows a decrease of 80%, while with the physical activation, this decrease stands at around 30%.

#### 4. Conclusions

Hydrogen sulphide removal performance of waste-derived material, such as biochar show lower adsorption capacity compared to optimized commercial sorbents. These results, although preliminary are important for the future optimization of waste-derived materials. In fact, such types of materials can be reinserted in the gas production cycle as fertilizer or structuring material for the anaerobic digestion process.

Physical activation with CO<sub>2</sub> and temperature promotes for activated biochar an adsorption capacity that increases with values comparable to commercial sorbents, while ashes performance are still too poor.

Humid biogas should be dried, because water enters into competition with hydrogen sulphide that has to be removed. A more pronounced decrease of adsorption capacities is recorded for not physically activated material. This is due to the higher competition between water content and trace compounds to be removed with low surface area and microporous volume.

**Supplementary Materials:** The following are available online at <http://www.mdpi.com/1996-1073/11/9/2338/s1>.

**Author Contributions:** S.F. for the chemical analysis and D.P. and M.S. for the research activity and for the supervision work.

**Acknowledgments:** This research is part of the BWS project (Biowaste for SOFCs) carried out with Fondazione Edmund Mach and SOLIDpower SpA. The project is funded by the contribution of Fondazione Caritro (TN). This research is also part of the DEMOSOFC project (European project FCH2 JU—grant number 671470) and BIOGAS4ENERGY (National project carried out with FinPiemonte).

**Conflicts of Interest:** The authors declare no conflict of interest.

## References

1. Torrijos, M. State of Development of Biogas Production in Europe. *Procedia Environ. Sci.* **2016**, *35*, 881–889. [[CrossRef](#)]
2. Papurello, D.; Soukoulis, C.; Schuhfried, E.; Cappellin, L.; Gasperi, F.; Silvestri, S.; Santarelli, M.; Biasioli, F. Monitoring of volatile compound emissions during dry anaerobic digestion of the Organic Fraction of Municipal Solid Waste by Proton Transfer Reaction Time-of-Flight Mass Spectrometry. *Bioresour. Technol.* **2012**, *126*. [[CrossRef](#)] [[PubMed](#)]
3. Papurello, D.; Lanzini, A. SOFC single cells fed by biogas: Experimental tests with trace contaminants. *Waste Manag.* **2017**. [[CrossRef](#)] [[PubMed](#)]
4. Papurello, D.; Silvestri, S.; Tomasi, L.; Belcari, I.; Biasioli, F.; Santarelli, M. Biowaste for SOFCs. *Energy Procedia* **2016**, *101*, 424–431. [[CrossRef](#)]
5. Rasi, S.; Veijanen, A.; Rintala, J. Trace compounds of biogas from different biogas production plants. *Energy* **2007**, *32*, 1375–1380. [[CrossRef](#)]
6. Rasi, S.; Lantela, J.; Rintala, J. Trace compounds affecting biogas energy utilisation—A review. *Energy Convers. Manag.* **2011**, *52*, 3369–3375. [[CrossRef](#)]
7. Van Foreest, F. *Perspectives for Biogas in Europe*; Oxford Institute for Energy Studies: Oxford, UK, 2012; ISBN 9781907555633.
8. Papurello, D.; Lanzini, A.; Tognana, L.; Silvestri, S.; Santarelli, M. Waste to energy: Exploitation of biogas from organic waste in a 500 W<sub>el</sub> solid oxide fuel cell (SOFC) stack. *Energy* **2015**, *85*. [[CrossRef](#)]
9. Kaparaju, P.; Rintala, J. Generation of heat and power from biogas for stationary applications: Boilers, gas engines and turbines, combined heat and power (CHP) plants and fuel cells. In *The Biogas Handbook, Science, Production and Applications*; Elsevier: New York, NY, USA, 2013; pp. 404–427.
10. Patrizio, P.; Leduc, S.; Chinese, D.; Dotzauer, E.; Kraxner, F. Biomethane as transport fuel—A comparison with other biogas utilization pathways in northern Italy. *Appl. Energy* **2015**, *157*, 25–34. [[CrossRef](#)]
11. Saldivia, A.; Mainero, D. Biomethane from OFMSW. In Proceedings of the Ecomondo, Rimini, Italy, 5–8 November 2014.
12. Facci, A.L.; Cigolotti, V.; Jannelli, E.; Ubertini, S. Technical and economic assessment of a SOFC-based energy system for combined cooling, heating and power. *Appl. Energy* **2016**. [[CrossRef](#)]
13. Choudhury, A.; Chandra, H.; Arora, A. Application of solid oxide fuel cell technology for power generation—A review. *Renew. Sustain. Energy Rev.* **2013**, *20*, 430–442. [[CrossRef](#)]
14. Papurello, D.; Borchellini, R.; Bareschino, P.; Chiodo, V.; Freni, S.; Lanzini, A.; Pepe, F.; Ortigoza, G.A.; Santarelli, M. Performance of a Solid Oxide Fuel Cell short-stack with biogas feeding. *Appl. Energy* **2014**, *125*. [[CrossRef](#)]
15. Papurello, D.; Lanzini, A.; Leone, P.; Santarelli, M. The effect of heavy tars (toluene and naphthalene) on the electrochemical performance of an anode-supported SOFC running on bio-syngas. *Renew. Energy* **2016**, *99*. [[CrossRef](#)]
16. Papurello, D.; Lanzini, A.; Drago, D.; Leone, P.; Santarelli, M. Limiting factors for planar solid oxide fuel cells under different trace compound concentrations. *Energy* **2016**, *95*. [[CrossRef](#)]

17. Lanzini, A.; Madi, H.; Chiodo, V.; Papurello, D.; Maisano, S.; Santarelli, M.; Van herle, J. Dealing with fuel contaminants in biogas-fed solid oxide fuel cell (SOFC) and molten carbonate fuel cell (MCFC) plants: Degradation of catalytic and electro-catalytic active surfaces and related gas purification methods. *Prog. Energy Combust. Sci.* **2017**, *61*, 150–188. [CrossRef]
18. Madi, H.; Lanzini, A.; Papurello, D.; Diethelm, S.; Ludwig, C.; Santarelli, M.; Van herle, J. Solid oxide fuel cell anode degradation by the effect of hydrogen chloride in stack and single cell environments. *J. Power Sources* **2016**, *326*, 349–356. [CrossRef]
19. Xu, C.; Gong, M.; Zondlo, J.W.; Liu, X.; Finklea, H.O. The effect of HCl in syngas on Ni-YSZ anode-supported solid oxide fuel cells. *J. Power Sources* **2010**, *195*, 2149–2158. [CrossRef]
20. Chen, H.; Wang, F.; Wang, W.; Chen, D.; Li, S.D.; Shao, Z. H<sub>2</sub>S poisoning effect and ways to improve sulfur tolerance of nickel cermet anodes operating on carbonaceous fuels. *Appl. Energy* **2016**, *179*, 765–777. [CrossRef]
21. Papurello, D.; Lanzini, A.; Fiorilli, S.; Smeacetto, F.; Singh, R.; Santarelli, M. Sulfur poisoning in Ni-anode solid oxide fuel cells (SOFCs): Deactivation in single cells and a stack. *Chem. Eng. J.* **2016**, *283*. [CrossRef]
22. Papurello, D.; Lanzini, A.; Leone, P.; Santarelli, M.; Silvestri, S. Biogas from the organic fraction of municipal solid waste: Dealing with contaminants for a solid oxide fuel cell energy generator. *Waste Manag.* **2014**, *34*, 2047–2056. [CrossRef] [PubMed]
23. Chiang, Y.-C.; Chiang, P.-C.; Huang, C.-P. Effects of pore structure and temperature on VOC adsorption on activated carbon. *Carbon* **2001**, *39*, 523–534. [CrossRef]
24. Papurello, D.; Schuhfried, E.; Lanzini, A.; Romano, A.; Cappellin, L.; Märk, T.D.; Silvestri, S.; Santarelli, M.; Biasioli, F. Proton transfer reaction-mass spectrometry as a rapid inline tool for filter efficiency of activated charcoal in support of the development of Solid Oxide Fuel Cells fueled with biogas. *Fuel Process. Technol.* **2015**, *130*. [CrossRef]
25. Papurello, D.; Tognana, L.; Lanzini, A.; Smeacetto, F.; Santarelli, M.; Belcari, I.; Silvestri, S.; Biasioli, F. Proton transfer reaction mass spectrometry technique for the monitoring of volatile sulfur compounds in a fuel cell quality clean-up system. *Fuel Process. Technol.* **2015**, *130*. [CrossRef]
26. Papurello, D.; Schuhfried, E.; Lanzini, A.; Romano, A.; Cappellin, L.; Märk, T.D.; Silvestri, S.; Biasioli, F. Influence of co-vapors on biogas filtration for fuel cells monitored with PTR-MS (Proton Transfer Reaction-Mass Spectrometry). *Fuel Process. Technol.* **2014**, *118*. [CrossRef]
27. Aksoylu, A.E.; Madalena, M.; Freitas, A.; Pereira, M.F.R.; Figueiredo, J.L. Effects of different activated carbon supports and support modifications on the properties of Pt/AC catalysts. *Carbon* **2001**, *39*, 175–185. [CrossRef]
28. Monteleone, G.; De Francesco, M.; Galli, S.; Marchetti, M.; Naticchioni, V. Deep H<sub>2</sub>S removal from biogas for molten carbonate fuel cell (MCFC) systems. *Chem. Eng. J.* **2011**, *173*, 407–414. [CrossRef]
29. Arnold, M. Reduction and Monitoring of Biogas Trace Compounds. Available online: <https://www.vtt.fi/inf/pdf/tiedotteet/2009/T2496.pdf> (accessed on 30 August 2018).
30. Barelli, L.; Bidini, G.; De Arespachoga, N.; Laura, P.; Sisani, E. Biogas use in high temperature fuel cells: Enhancement of KOH-KI activated carbon performance toward H<sub>2</sub>S removal. *Int. J. Hydrogen Energy* **2017**, *42*, 10341–10353. [CrossRef]
31. Papurello, D.; Tomasi, L.; Silvestri, S.; Santarelli, M. Evaluation of the Wheeler-Jonas parameters for biogas trace compounds removal with activated carbons. *Fuel Process. Technol.* **2016**, *152*. [CrossRef]
32. Papurello, D.; Tomasi, L.; Silvestri, S. Proton transfer reaction mass spectrometry for the gas cleaning using commercial and waste-derived materials: Focus on the siloxane removal for SOFC applications. *Int. J. Mass Spectrom.* **2018**, *430*. [CrossRef]
33. Erto, A.; Chianese, S.; Lancia, A.; Musmarra, D. On the mechanism of benzene and toluene adsorption in single-compound and binary systems: Energetic interactions and competitive effects. *Desalin. Water Treat.* **2017**, *86*, 259–265. [CrossRef]
34. Karatza, D.; Lancia, A.; Musmarra, D.; Pepe, F.; Volpicelli, G. Removal of mercuric chloride from flue gas by sulfur impregnated activated carbon. *Hazard. Waste Hazard. Mater.* **1996**, *13*, 95–105. [CrossRef]
35. Papurello, D.; Silvestri, S.; Lanzini, A. Biogas cleaning: Trace compounds removal with model validation. *Sep. Purif. Technol.* **2018**, *210*, 80–92. [CrossRef]
36. Ayse, E.; Nurgul, O.; Eylem, P.O.; Ersan, P. Fixed-bed pyrolysis of cotton stalk for liquid and solid products. *Fuel Process. Technol.* **2005**, *86*, 1207–1219. [CrossRef]

37. Shang, G.; Li, Q.; Liu, L.; Chen, P.; Huang, X. Adsorption of hydrogen sulfide by biochars derived from pyrolysis of different agricultural/forestry wastes. *J. Air Waste Manag. Assoc.* **2016**, *66*, 8–16. [[CrossRef](#)] [[PubMed](#)]
38. Gutiérrez Ortiz, F.J.; Aguilera, P.G.; Ollero, P. Biogas desulfurization by adsorption on thermally treated sewage-sludge. *Sep. Purif. Technol.* **2014**, *123*, 200–213. [[CrossRef](#)]
39. Paparello, D.; Tomasi, L.; Silvestri, S.; Belcari, I.; Santarelli, M.; Smeacetto, F.; Biasioli, F. Biogas trace compound removal with ashes using proton transfer reaction time-of-flight mass spectrometry as innovative detection tool. *Fuel Process. Technol.* **2016**, *145*. [[CrossRef](#)]
40. Ducom, G.; Radu-Tirnovanu, D.; Pascual, C.; Benadda, B.; Germain, P.; Kwong, C.W.; Chao, C.Y.H.; Subramanian, S.; Pande, G.; De Weireld, G.; et al. Sugarcane bagasse fly ash as an attractive agro-industry source for VOC removal on porous carbon. *J. Hazard. Mater.* **2013**, *49*, 683–690. [[CrossRef](#)]
41. Sigot, L.; Ducom, G.; Benadda, B.; Labouré, C. Comparison of adsorbents for H<sub>2</sub>S and D4 removal for biogas conversion in a solid oxide fuel cell. *Environ. Technol.* **2016**, *37*, 86–95. [[CrossRef](#)] [[PubMed](#)]
42. Ducom, G.; Radu-Tirnovanu, D.; Pascual, C.; Benadda, B.; Germain, P. Biogas—Municipal solid waste incinerator bottom ash interactions: Sulphur compounds removal. *J. Hazard. Mater.* **2009**, *166*, 1102–1108. [[CrossRef](#)] [[PubMed](#)]
43. Kastner, J.R.; Das, K.C.; Buquoi, Q.; Melear, N.D. Low temperature catalytic oxidation of hydrogen sulfide and methanethiol using wood and coal fly ash. *Environ. Sci. Technol.* **2003**, *37*, 2568–2574. [[CrossRef](#)] [[PubMed](#)]
44. Paparello, D.; Boschetti, A.; Silvestri, S.; Khomenko, I.; Biasioli, F. Real-time monitoring of removal of trace compounds with PTR-MS: Biochar experimental investigation. *Renew. Energy* **2018**, *125*. [[CrossRef](#)]
45. De Arespacochaga, N.; Valderrama, C.; Mesa, C.; Bouchy, L.; Cortina, J.L. Biogas deep clean-up based on adsorption technologies for Solid Oxide Fuel Cell applications. *Chem. Eng. J.* **2014**, *255*, 593–603. [[CrossRef](#)]
46. Beeckman, J.W.L.; Fassbender, N.A.; Datz, T.E. Length to Diameter Ratio of Extrudates in Catalyst Technology I. Modeling Catalyst Breakage by Impulsive Forces. *AIChE J.* **2016**, *62*, 639–647. [[CrossRef](#)]
47. Barelli, L.; Bidini, G.; Hern, E.; Sisani, E.; Alvarez, J.M. Performance characterization of a novel Fe-based sorbent for anaerobic gas desulfurization finalized to high temperature fuel cell applications. *Int. J. Hydrogen Energy* **2017**, *42*, 1859–1874. [[CrossRef](#)]
48. Tepper, F.; King, J.; Greer, J. The Alkali metal. In Proceedings of the Chemical Society, London, UK, 19–22 July 1967.
49. Richardson, J.; Bjorheden, R.; Hakkala, P.; Lowe, A.T.; Smith, C.T. *Bioenergy from Sustainable Forestry—Guiding Principles and Practice*; Kluwer Academic Publisher: New York, NY, USA; Boston, MA, USA; Dordrecht, The Netherlands; London, UK; Moscow, Russia, 2002; ISBN 0306475197.
50. Wei, L.; Yushin, G. Nanostructured activated carbons from natural precursors for electrical double layer capacitors. *Nano Energy* **2012**, *1*, 552–565. [[CrossRef](#)]
51. Yahya, M.A.; Al-Qodah, Z.; Ngah, C.W.Z. Agricultural bio-waste materials as potential sustainable precursors used for activated carbon production: A review. *Renew. Sustain. Energy Rev.* **2015**, *46*, 218–235. [[CrossRef](#)]
52. Williams, P.T.; Reed, A.R. Pre-formed activated carbon matting derived from the pyrolysis of biomass natural fibre textile waste. *J. Anal. Appl. Pyrolysis* **2003**, *70*, 563–577. [[CrossRef](#)]
53. Williams, P.T.; Reed, A.R. Development of activated carbon pore structure via physical and chemical activation of biomass fibre waste. *Biomass Bioenergy* **2006**, *30*, 144–152. [[CrossRef](#)]
54. Yang, C.; Liu, Y. Preparing Desirable Activated Carbons from Agricultural Residues for Potential Uses in Water Treatment. *Waste Biomass Valoriz.* **2015**, *6*, 1029–1036. [[CrossRef](#)]
55. Nabais, V.J.M.; Nunes, P.; Carrott, P.J.M.; Ribeiro, M.M.L.; García, A.M.; Díaz-díez, M.A. Production of activated carbons from coffee endocarp by CO<sub>2</sub> and steam activation. *Fuel Process. Technol.* **2007**, *9*. [[CrossRef](#)]
56. Zhang, T.; Walawender, W.P.; Fan, L.T.; Fan, M.; Daugaard, D.; Brown, R.C. Preparation of activated carbon from forest and agricultural residues through CO<sub>2</sub> activation. *Chem. Eng. J.* **2004**, *105*, 53–59. [[CrossRef](#)]
57. Guo, S.; Peng, J.; Li, W.; Yang, K.; Zhang, L.; Zhang, S.; Xia, H. Effects of CO<sub>2</sub> activation on porous structures of coconut shell-based activated carbons. *Appl. Surface Sci.* **2009**, *255*, 8443–8449. [[CrossRef](#)]
58. Cha, J.S.; Park, S.H.; Jung, S.; Ryu, C.; Jeon, J.; Shin, M.; Park, Y. Journal of Industrial and Engineering Chemistry Production and utilization of biochar: A review. *J. Ind. Eng. Chem.* **2016**, *40*, 1–15. [[CrossRef](#)]

59. Adib, F.; Bagreev, A.; Bandosz, T.J. Analysis of the Relationship between H<sub>2</sub>S Removal Capacity and Surface Properties of Unimpregnated Activated Carbons. *Environ. Sci. Technol.* **2000**, *34*, 686–692. [[CrossRef](#)]
60. Aravind, P.V.; De Jong, W. Evaluation of high temperature gas cleaning options for biomass gasification product gas for Solid Oxide Fuel Cells. *Prog. Energy Combust. Sci.* **2012**, *38*, 737–764. [[CrossRef](#)]
61. Sethupathi, S.; Zhang, M.; Rajapaksha, A.U.; Lee, S.R.; Nor, N.M.; Mohamed, A.R.; Al-Wabel, M.; Lee, S.S.; Ok, Y.S. Biochars as potential adsorbents of CH<sub>4</sub>, CO<sub>2</sub> and H<sub>2</sub>S. *Sustainability* **2017**, *9*, 121. [[CrossRef](#)]
62. Xue, M.; Chitrakar, R.; Sakane, K.; Ooi, K. Screening of adsorbents for removal of H<sub>2</sub>S at room temperature. *Green Chem.* **2003**, *5*, 529–534. [[CrossRef](#)]
63. Wood, G.O. Activated carbon adsorption capacities for vapors. *Carbon* **1992**, *30*, 593–599. [[CrossRef](#)]



© 2018 by the authors. Licensee MDPI, Basel, Switzerland. This article is an open access article distributed under the terms and conditions of the Creative Commons Attribution (CC BY) license (<http://creativecommons.org/licenses/by/4.0/>).